HOUSE SST271

Semicond. Sci. Technol. 5 (1990) 000–000. Printed in the UK

Matrix elements for hole–phonon scattering in a semiconductor quantum well

R W Kelsall, R I Taylor†, A C G Wood and R A Abram

Applied Physics Group, School of Engineering and Applied Science, University of Durham, South Road, Durham DH1 3LE, UK

Received 1 December 1989, accepted for publication 12 April 1989

Abstract. Matrix elements for hole–phonon scattering in a quantum well are calculated using a four-band $\boldsymbol{k}\cdot\boldsymbol{p}$ method. The method provides a realistic description of the quantum confined valence states, including the effects of heavy–light hole mixing. This mixing precludes the operation of any symmetry rules for phonon scattering, and the matrix elements are dependent on the specific character of the scattering states involved. For optical phonons, the matrix elements exhibit a strong dependence on the in-plane wavevectors of the scattering states, especially for states lying near the so-called anticrossing regions of the valence subbands. For acoustic (deformation potential) phonons, the matrix elements for intrasubband processes are relatively independent of the in-plane wavevector. In both cases, the larger matrix elements are generally those for intrasubband scattering, with the dominant intersubband processes being those involving adjacent and anticrossing bands.

1. Introduction

An understanding of the interaction between electrons and phonons forms an essential part of any study of carrier transport phenomena in semiconductors. The same is true of transport in quantum confined semiconductor structures (super lattices and quantum wells) in which both carriers and phonons occupy quasi-two-dimensional (2D) states. Analyses of the electron–phonon interaction in the conduction bands of such structures have already been presented [1–3]; however, the corresponding hole–phonon scattering processes in the valence bands of quasi-2D systems have received relatively little attention. This is presumably due to the complexity of the quantum confined valence bandstructure. In a quasi-2D semiconductor structure, mixing of the heavy and light hole states occurs [4,5], giving rise to a set of subbands whose energy dispersion in the plane of the 2D layers is markedly non-parabolic. The character of the valence states shows a strong dependence on the in-plane wavevector, and a description of these states by a simple one-band effective mass model — as is commonly used for the conduction band system — is no longer appropriate.

The purpose of this paper is to show how the matrix elements for hole–phonon scattering in a quasi-2D system are modified by these mixing effects. The work reported here represents the first stage of our development of a Monte Carlo simulation of hole dynamics in quantum wells [6]. Subsequent stages of this work will be reported in a series of forthcoming publications. In section 2 of this paper we will set out a model calculation of the hole–phonon scattering matrix elements, using a four-band $\boldsymbol{k}\cdot\boldsymbol{p}$ scheme to describe the quantum confined valence states. We will consider the following cases: scattering by acoustic phonons (via the deformation potential interaction), and by optical phonons (via the deformation potential and Fröhlich interactions). We will refer to these processes as 'acoustic', 'non-polar optical' scattering, respectively. In section 3 we will present results for intra- and inter-subband transitions via the above processes for the specific case of a 100 Å GaAs/AlAs quantum well.

2. Theory

For the purposes of this model calculation, we will assume that the phonon modes in the quantum well can be taken to be bulk-like. In this respect, our work will be complementary to that of Price [1], and Ridley and co-workers [2,3], who calculated phonon scattering matrix elements for conduction electrons in a quasi-2D structure, using a confined electron–bulk phonon model. However we acknowledge that, for a more exact treatment, confined phonon states should be used [7].

In the bulk phonon approximation, calculation of the

† Present address: Plessey Research Caswell Limited, Allen Clark Research Centre, Towcester, Northants, UK.

matrix elements for any carrier–phonon scattering process involves the evaluation of the integral

$$I(k', k) = \int \psi_{k'}^*(r) \exp(\pm i q \cdot r) \psi_k(r) \mathrm{d}r \qquad (1)$$

where $\psi_k(r)$ is the carrier wavefunction in the quantum well, k and k' are the wavevectors of the initial and final carrier states, and q is the phonon wavevector. In general, the upper sign in the exponential term should be taken for phonon absorption and the lower sign for emission.

To determine the valence states, we have used the 4-band $k \cdot p$ scheme of Schuurmans and 't Hooft [8], extended to include spin effects as described by Eppenga *et al* [9]. In this approach, the quantum well wavefunctions ψ are taken as linear combinations of bulk wavefunctions φi

$$\psi = \sum_i A_i \varphi_i \qquad (2)$$

where the φ_i are sums over plane waves

$$\varphi_i = \sum_j U_{ij} \exp(i k_i \cdot r) u_j(r). \qquad (3)$$

The $u_j(r)$ are the $k \cdot p$ basis set consisting of zone centre Bloch states for the lowest conduction band, the heavy, light and spin split-off hole bands, for both spin parities; eight basis states in all.

Solutions of the Schrödinger equation are sought in the three regions of the quantum well: $[-\infty, L/2]$, region I; $[-L/2, L/2]$, region II, and $[L/2, \infty]$, region III (L is the quantum well width), with continuity of the carrier wavefunction and the probability current required at the interfaces. Continuity of ψ means that $K_{\parallel}$ must be the same in all three regions, and hence the quantum well wavefunction in region I can be written as

$$\psi \mathrm{I}(r) = \exp(i k_{\parallel} \cdot r_{\parallel}) \sum_{ij} A_i^{\mathrm{I}} U_{ij}^{\mathrm{I}} u_j(r) \exp(i k_{z,i}^{\mathrm{I}} z). \qquad (4)$$

ψ_{II} and ψ_{III} take exactly the same form, with the basis states $u_j(r)$ assumed to be the same in both well and barrier regions.

Consequently, $I(k', k)$ consists of three terms, which we shall denote I_{I}, I_{II} and I_{III}, each similar in form to equation (1), but with the limits of integration defined by the boundaries of regions I, II and III as given above. In this calculation, we will assume for simplicity, that the phonon modes are bulk GaAs-like in all three regions of the quantum well system. In practice, the contribution to the matrix elements from the barrier regions will be small, and the choice of phonon modes in these regions will not have any significant effect on the results.

We will consider firstly the term I_{II}. Let the wavefunctions of the initial and final states in region II be

$$\psi_{A,\mathrm{II}}(r) = \exp(i k_{\parallel}^A \cdot r_{\parallel}) \sum_{ij} A_i^{\mathrm{II}} U_{ij}^{\mathrm{II}} u_j(r) \exp(i k_{z,i}^{A\mathrm{II}} z), \qquad (5a)$$

$$\psi_{B,\mathrm{II}}(r) = \exp(i k_{\parallel}^B \cdot r_{\parallel}) \sum_{lk} B_l^{\mathrm{II}} V_{lk}^{\mathrm{II}} u_k(r) \exp(i k_{z,l}^{B\mathrm{II}} z), \qquad (5b)$$

Substituting these equations into equation (1) gives

$$I_{\mathrm{II}}, BA = \sum_{ijlk} A_i^{\mathrm{II}} U_{ij}^{\mathrm{II}} B_l^{*\mathrm{II}} V_{lk}^{*\mathrm{II}} \times \int_{z=-L/2}^{z=L/2} \exp[i(k_{\parallel}^A - k_{\parallel}^{*B} \pm q_{\parallel}) \cdot r_{\parallel}] \times u_j(r) u_k^*(r) \exp[i(k_{z,i}^{A\mathrm{II}} - k_{z,l}^{*B\mathrm{II}} \pm q_z) z] \mathrm{d}r. \qquad (6)$$

The product $u_j(r) u_k^*(r)$ can be expanded as a Fourier series over reciprocal lattice vectors:

$$u_j(r) u_k^*(r) = \sum_g c_{g,jk} \exp(i g \cdot r) \qquad (7)$$

where

$$c_{g,jk} = \frac{1}{\Omega} \int_{\mathrm{cell}} u_j(r) u_k^*(r) \exp(-i g \cdot r) \mathrm{d}r \qquad (8)$$

with Ω the unit cell volume.

We now write $\mathrm{d}r = \mathrm{d}r_{\parallel}\, \mathrm{d}z$ and integrate over $r_{\parallel}$ to obtain

$$I_{\mathrm{II}}, BA = (2\pi)^2 \sum_g c_{g,jk} \delta(k_{\parallel}^A - k_{\parallel}^B + g_{\parallel} \pm q_{\parallel}) \times \sum_{ijlk} A_i^{\mathrm{II}} U_{ij}^{\mathrm{II}} B_l^{*\mathrm{II}} V_{lk}^{*\mathrm{II}} \int_{-L/2}^{L/2} \exp[i(k_{z,i}^{A\mathrm{II}} - k_{z,l}^{*B\mathrm{II}} + g_z \pm q_z) z] \mathrm{d}z \qquad (9)$$

where we have assumed that $k_{\parallel}^A$ and $k_{\parallel}^B$ are real, since evanescent solutions are not expected in the plane of the quantum well.

The smallest allowed values of $g_{\parallel}$ will be much larger than the typical values of in-plane carrier wavevectors $k_{\parallel}^A$ and $k_{\parallel}^B$, and therefore only the terms with $g_{\parallel} = 0$ will contribute significantly to the sum over g. Similarly, the allowed values of g_z will all be considerably larger than the carrier wavevector components $k_z \sim \pi/L$, resulting in very small values of the integral over z for $g_z \neq 0$. Therefore, we may, to a good approximation, neglect all but the $g = 0$ term in the sum. From equation (8), the coefficient of this term is $c_{0,jk} = \delta_{j,k}$, since the bulk basis states form an orthogonal set. Then, carrying out the integral over z, we obtain the result

$$I_{\mathrm{II},BA} = L(2\pi)^2 \delta(k_{\parallel}^A - k_{\parallel}^B \pm q_{\parallel}) \sum_{ijl} A_i^{\mathrm{II}} U_{ij}^{\mathrm{II}} B_l^{*\mathrm{II}} V_{lj}^{*\mathrm{II}} \times \frac{\sin(k_{z,i}^{A\mathrm{II}} - k_{z,l}^{*B\mathrm{II}} \pm q_z) L/2}{(k_{z,i}^{A\mathrm{II}} - k_{z,l}^{*B\mathrm{II}} \pm q_z) L/2}. \qquad (10)$$

Secondly, we will consider I_{I}. The mathematical form of the wavefunctions is the same as for I_{II}. However, we know that the real parts of the wavevectors $k_{z,i}^{A\mathrm{I}}$ and $k_{z,l}^{B\mathrm{I}}$ will always be zero, since no oscillatory solutions are allowed in the barrier regions. Furthermore, for region I, only those wavevectors with *negative* imaginary parts are allowed (to ensure $\psi \to 0$ as $z \to -\infty$). Thus we can write the wavefunctions in region I in the form

$$\psi_{A,\mathrm{I}}(r) = \exp(i k_{\parallel}^A \cdot r_{\parallel}) \sum_{ij} A_i^{\mathrm{I}} U_{ij}^{\mathrm{I}} u_j(r) \exp(\kappa_{z,i}^{A\mathrm{I}} z) \qquad (11a)$$

$$\psi_{B,\mathrm{I}}(r) = \exp(i k_{\parallel}^B \cdot r_{\parallel}) \sum_{lk} B_l^{\mathrm{I}} V_{lk}^{\mathrm{I}} u_k(r) \exp(\kappa_{z,l}^{B\mathrm{I}} z) \qquad (11b)$$

where $\kappa_{z,i}^{A_I} = -\mathrm{Im}(k_{z,i}^{A_I})$, $\kappa_{z,l}^{B_I} = -\mathrm{Im}(k_{z,l}^{B_I})$, and the A_i^I and B_l^I are the coefficients of a subset of exactly half the bulk basis states in region I. We then obtain for I_I:

$$I_{I,BA} = L(2\pi)^2\delta(k_\parallel^A - k_\parallel^B \pm q_\parallel)\sum_{ijl} A_i^I U_{ij}^I B_l^{*I} V_{lj}^{*I} \times \frac{1}{2}\frac{\exp[-(\kappa_{z,i}^{A_I} + \kappa_{z,l}^{B_I} \pm iq_z)L/2]}{(\kappa_{z,i}^{A_I} + \kappa_{z,l}^{B_I} \pm iq_z)L/2}. \quad (12)$$

For region III, again the real parts of the $\kappa_{z,i}^{A_{III}}$, $\kappa_{z,l}^{B_{III}}$ will be zero, but this time only wavevectors with positive imaginary parts are allowed. Thus

$$I_{III,BA} = L(2\pi)^2\delta(k_\parallel^A - k_\parallel^B \pm q_\parallel)\sum_{ijl} A_i^{III} U_{ij}^{III} B_l^{*III} V_{lj}^{*III} \times \frac{1}{2}\frac{\exp[-(\kappa_{z,i}^{A_{III}} + \kappa_{z,l}^{B_{III}} \mp iq_z)L/2]}{(\kappa_{z,i}^{A_{III}} + \kappa_{z,l}^{B_{III}} \mp iq_z)L/2} \quad (13)$$

where $\kappa_{z,i}^{A_{III}} = \mathrm{Im}(k_{z,i}^{A_{III}})$ and $\kappa_{z,l}^{B_{III}} = \mathrm{Im}(k_{z,l}^{B_{III}})$.

Collecting together the results of equations (10), (12) and (13), we obtain

$$|I_{BA}|^2 = |I_{I,BA} + I_{II,BA} + I_{III,BA}|^2. \quad (14)$$

This result should be modified to account for normalisation of the carrier wavefunctions, i.e. we require

$$|I'_{BA}|^2 = \frac{|I_{BA}|^2}{N_A N_B} \quad (15)$$

where $N_A = \int \psi_A^* \psi_A \, \mathrm{d}r$. This gives

$$|I'_{BA}|^2 = \frac{(2\pi)^2}{\mathscr{A}}\delta(k_\parallel^A - k_\parallel^B \pm q_\parallel)|J_{BA}(q_z)|^2 \quad (16)$$

where $\mathscr{A}$ is the area of the quantum well plane, and the term $|J_{BA}(q_z)|^2$ contains all the details of the interaction of the quantum confined hole states with the phonon mode in the z direction.

For carrier–phonon scattering in a quantum well, a general expression for the scattering rate can be derived from Fermi's Golden Rule:

$$P_{n',n}(k_\parallel) = \frac{2\pi}{\hbar}\frac{\Omega}{(2\pi)^3}\iint \delta_{k_\parallel \pm q_\parallel, k'_\parallel}\left(\frac{\hbar}{2M'\omega_q}\right)\begin{bmatrix}\mathcal{N}_q \\ \mathcal{N}_q + 1\end{bmatrix} C_q^2 \times |J_{k'_\parallel n', k_\parallel n}(q_z)|^2 \delta[\epsilon(k'_\parallel, n') - \epsilon(k_\parallel, n) \mp \epsilon_{ph}]\mathrm{d}k'_\parallel \, \mathrm{d}q_z \quad (17)$$

where M' is the lattice oscillator mass, ω_q is the phonon frequency of mode q, $\mathcal{N}_q$ is the phonon occupation number, ϵ_{ph} is the phonon energy, $\epsilon(k_\parallel, n)$ is the kinetic energy of a carrier in subband n, and C_q is a coupling coefficient for the particular scattering process. The upper case gives the result for phonon absorption, and the lower case, that for emission. We will assume that the subband energy dispersions are isotropic in the $k_\parallel$ plane. Consequently, the term $J_{k'_\parallel n', k_\parallel n}(q_z)$ will also be independent of the directions of $k_\parallel$ and $k'_\parallel$.

For acoustic scattering in the elastic and energy equipartition approximations we obtain the result:

$$P_{n',n}(k_\parallel) = P_{AC}\iint \delta_{k_\parallel \pm q_\parallel, k_\parallel}|J_{k'_\parallel n', k_\parallel n}(q_z)|^2 \times \delta\Big(\epsilon(k'_\parallel, n) - \epsilon(k_\parallel, n)\Big)\mathrm{d}k'_\parallel \mathrm{d}q_z = P_{AC}D_{n'}(k'_\parallel)M^2_{k'_\parallel n', k_\parallel n} \quad (18)$$

where

$$P_{AC} = \frac{k_B T E_{AC}^2}{8\pi^2\hbar\rho v_s^2} \quad (19)$$

with E_{AC} the acoustic deformation potential in the quantum well, ρ the crystal density, and v_s the crystal sound velocity. $D_{n'}(k'_\parallel)$ is the density of states in subband n'

$$D_{n'}(k'_\parallel) = 2\pi\left|\frac{k_\parallel}{\delta\epsilon/\delta k_\parallel}\right|_{k_\parallel = k'_\parallel} \quad (20)$$

and

$$M^2_{k'_\parallel n', k_\parallel n} = \int |J_{k'_\parallel n', k_\parallel n}(q_z)|^2 \, \mathrm{d}q_z \quad (21)$$

where $k'_\parallel$ satisfies $\epsilon(k'_\parallel, n)$.

For non-polar optical scattering, following the treatment of Ridley [10] in which LO and TO phonons are assigned a common, q independent frequency ω_{op}, we obtain

$$P_{n',n}(k_\parallel) = P_{NPO}\begin{bmatrix}\mathcal{N}_{op} \\ \mathcal{N}_{op} + 1\end{bmatrix} D_{n'}(k'_\parallel)M^2_{k'_\parallel n', k_\parallel n} \quad (22)$$

where

$$P_{NPO} = \frac{D_{op}^2}{8\pi^2\rho\omega_{op}} \quad (23)$$

D_{op} is the optical deformation potential constant, and $\mathcal{N}_{op} = 1/[\exp(\hbar\omega_{op}/k_B T) - 1]$. Here, $k'_\parallel$ satisfies $\epsilon(k'_\parallel, n') = \epsilon(k_\parallel, n) \pm \hbar\omega_{op}$.

For polar optical scattering, via the Fröhlich interaction [11,12], we find

$$P_{n',n}(k_\parallel) = P_{POP}\begin{bmatrix}\mathcal{N}_{op} \\ \mathcal{N}_{op} + 1\end{bmatrix} D_{n'}(k'_\parallel)M^2_{k'_\parallel n', k_\parallel n} \quad (24)$$

where

$$P_{POP} = \frac{e^2\omega_{op}}{16\pi^3\varepsilon_0}\left(\frac{1}{\varepsilon_\infty} - \frac{1}{\varepsilon_s}\right) \quad (25)$$

with ε_s and ε_∞ the static and high frequency dielectric constants, and

$$M^2_{k'_\parallel n', k_\parallel n} = \iint \delta_{k_\parallel \pm q_\parallel, k'_\parallel}\frac{|J_{k'_\parallel n', k_\parallel n}(q_z)|^2}{q_\parallel^2 + q_z^2}\mathrm{d}q_z \, d\theta \quad (26)$$

with θ the angle between $k_\parallel$ and $k'_\parallel$. Integration over θ then gives

$$M^2_{k'_\parallel n', k_\parallel n} = 2\pi\int \frac{|J_{k'_\parallel n', k_\parallel n}(q_z)|^2}{\sqrt{[q_z^4 + 2(k_\parallel^2 + k_\parallel'^2)q_z^2 + (k_\parallel^2 - k_\parallel'^2)^2}}\mathrm{d}q_z \quad (27)$$

It is also possible to derive matrix elements for scattering by acoustic phonons via the piezoelectric interaction, using the approach detailed above. However, for such a calculation, additional aspects such as free carrier screening and the anisotropy of the coupling coefficient must be considered, and therefore we will defer any treatment of this process to a later publication.

3. Results and Discussion

We have calculated the terms M^2 for scattering by acoustic (AC), non-polar optical (NPO) and polar optical (POP) phonons, as detailed above, for holes in a 100 Å GaAs/AlAs quantum well. Figure 1 shows the in-plane dispersion of the first four valence subbands in the well. These subbands were obtained from a 4-band $k \cdot p$ calculation, using parameters taken from reference [8]. The effects of heavy hole–light hole mixing are clearly apparent; the subbands are distorted, with repulsion (anticrossing) phenomena visible between adjacent bands. These anticrossing regions are indicative of an exchange of character of the states in the pairs of subbands. The subbands are usually labelled according to the character of the (unmixed) zone centre states — hence the labelling HH1, HH2, LH1 and HH3 in figure 1 — however, for simplicity, we will refer simply to bands 1–4. The extent of the band mixing is such that all states $k_{\parallel} > 0$ are a hybrid of the zone centre states for all neighbouring subbands. This means that no symmetry rules can be deduced for either intra- or inter-band phonon scattering; the matrix elements are dependent on the specific nature of the initial and final states involved.

In Figures 2–4 we have shown the matrix elements squared for a selection of non-polar optical scattering processes within the four bands, as a function of $k_{\parallel}$, the wavevector of the lower energy state. Figures 5–7 show results for the same set of transitions for scattering by polar optical phonons. The optical phonon energy in both cases was taken as 36 meV, the LO phonon energy for GaAs.

Clearly, the matrix elements vary strongly with the wavevectors of the scattering states. This is in marked contrast to the case of NPO scattering of electrons in a

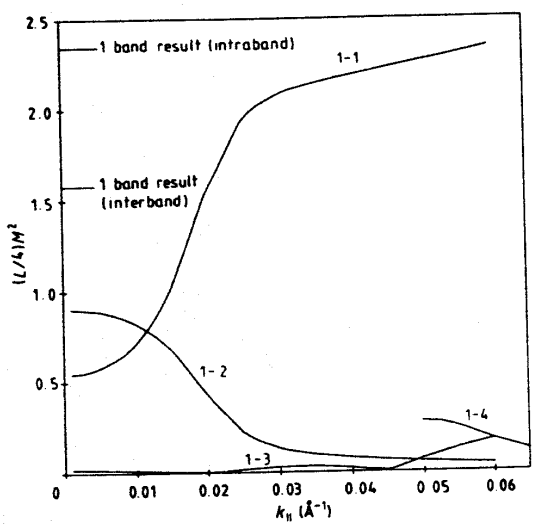

Figure 2. Matrix elements squared for NPO scattering as a function of the in-plane wavevector of the lower energy state, for processes in which the lower energy state is in band 1. The matrix elements squared are plotted in dimensionless form, $(L/4)\ M^2$, where M^2 is given by equation (21). Also shown are the results obtained for both intra- and inter-band scattering using a 1-band effective mass model.

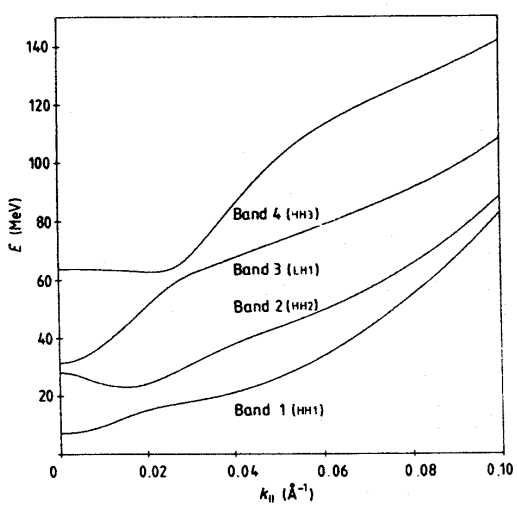

Figure 1. In-plane energy dispersion of the first four valence subbands of a 100 Å GaAs/AlAs quantum well. Zero energy corresponds to the base of the valence band well, and energy is measured as positive in the direction of increasing subband index.

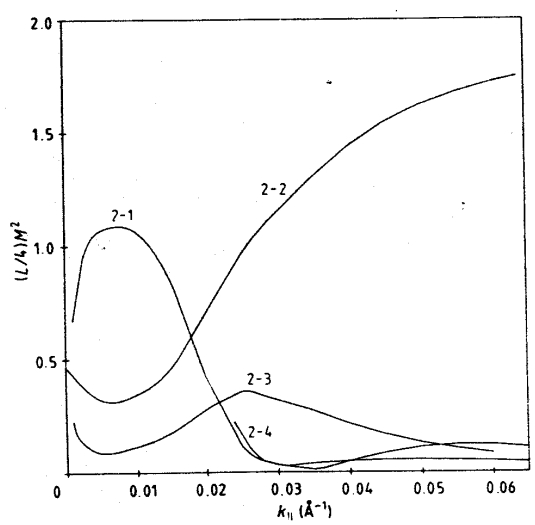

Figure 3. Matrix elements squared for NPO scattering for processes in which the lower energy state is in band 2, against in-plane wavevector in band 2.

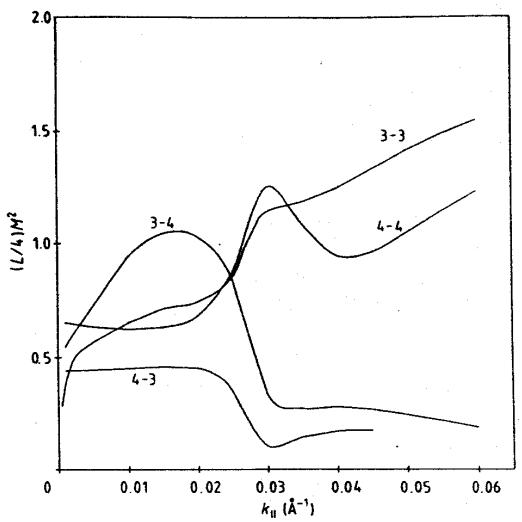

Figure 4. Matrix elements squared for NPO scattering in bands 3 and 4, as a function of the in-plane wavevector of the lower energy state. In the labels *n–m*, the subband index of the lower energy state is given by *n*.

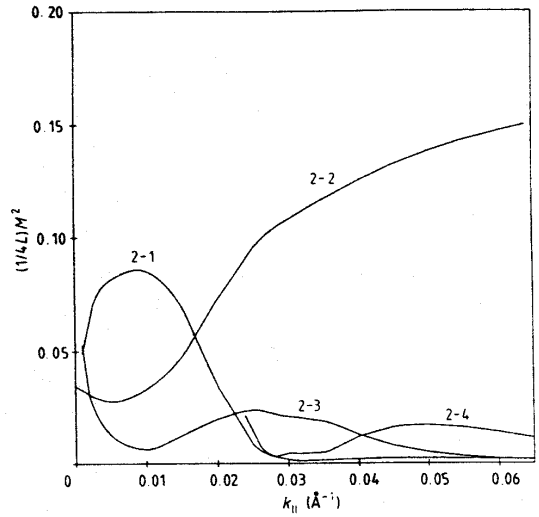

Figure 6. Matrix elements squared for POP scattering for processes in which the lower energy state is in band 2, against in-plane wavevector in band 2.

quantum well, which, when treated within a one-band effective mass approach [1,2], gives a fixed, k-independent value for the matrix element for all intrasubband transitions, and another fixed value for all intersubband transitions (see figure 2).

For the intraband processes NPO 1-1 and NPO 2-2 (figures 2 and 3 respectively), M^2 is small for small $k_{\parallel}$ and large for large $k_{\parallel}$. This is because, at small $k_{\parallel}$, the scattering states lie on opposite sides of the anticrossing region of bands 1 and 2, and are therefore quite dissimilar in character, giving rise to a small matrix element.

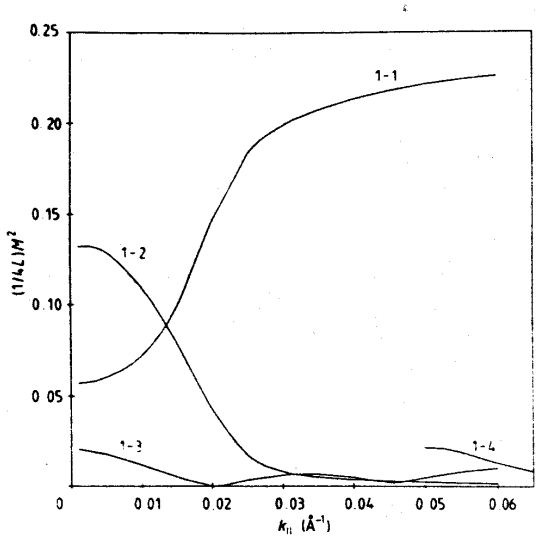

Figure 5. Matrix elements squared for POP scattering for processes in which the lower energy state is in band 1, against in-plane wavevector in band 1. The matrix elements squared are plotted in dimensionless form, $(1/4L)M^2$, where M^2 is given by equation (27).

However, as the wavevector of the lower energy state increases, the character of that state becomes much more like that of the upper energy state, until, for $k_{\parallel}$ well beyond the anticrossing region, the two states are very similar in character, and the scattering matrix element is large. Indeed, it can be seen from figure 2 that the intraband NPO matrix elements approach the 1-band effective mass result at large $k_{\parallel}$.

For interband scattering between two bands which exhibit the anticrossing effect, the converse trend is observed. This is illustrated by the results for NPO 1-2 and NPO 2-1 scattering in figures 2 and 3. At small $k_{\parallel}$, the upper and lower energy states are located on opposite

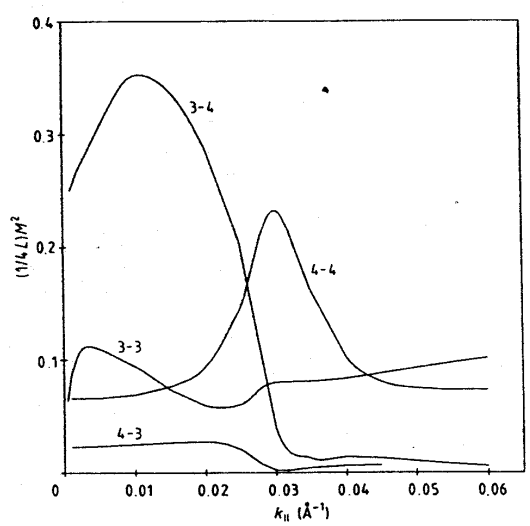

Figure 7. Matrix elements squared for POP scattering in bands 3 and 4, as a function of the in-plane wavevector of the lower energy state.

sides of the anticrossing region: because of the exchange of character which occurs, these states are similar in character, resulting in a large scattering matrix element. As $k_{\parallel}$ increases, the character of the lower energy state becomes less similar to that of the upper state, and the matrix element decreases. The same effect can be seen for NPO 3–4 and NPO 4–3 scattering on figures 4 and 5, respectively.

The results for POP scattering follow the basic trends described above, but with modifications due to the $1/q^2$ dependence of the Fröhlich interaction, although this dependence is smeared out somewhat, in the term M^2, by the integration over scattering angle θ (see equation (26)). (In the 1-band effective mass calculation, variations of M^2 with $k_{\parallel}$ arise solely from this $1/q^2$ dependence [1, 2].) One important consequence of the $1/q^2$ dependence can be seen in the relative magnitudes of the interband matrix elements. It is clear from figures 2–4, that the dominant interband matrix elements NPO scattering are those involving states in adjacent anticrossing bands. The matrix elements for the other interband processes shown are all considerably smaller. However, this is not universally true for POP scattering. In figure 7 it can be seen that the POP 4–3 matrix element is considerably smaller than the other matrix elements shown, and this is due to the large separation of the scattering states in k-space, for all $k_{\parallel}$. This means that the minimum value of phonon wavevector, $q_{\min} = |k_{\parallel} - k'_{\parallel}|$ is large; thus reducing the magnitude of the matrix element. Conversely, for POP 3–4 scattering at small $k_{\parallel}$, $q_{\min}$ is very small, giving rise to larger matrix elements than for any other POP process.

In figure 8 we have shown a plot of M^2 against $k_{\parallel}$ for a selection of AC scattering processes. The matrix elements for the four intraband processes shown as full curves in figure 8 are large (compared to those for NPO scattering) and vary only weakly with wavevector. This is because, in the approximation of elastic scattering, the initial and final states are identical for a given $k_{\parallel}$. In reality, the acoustic phonon energies are typically only of the order of 1 meV, in which the case the scattering states will still lie close together in k-space, preserving the general features shown for intraband scattering in figure 8. We have confirmed this argument by calculating matrix elements for the AC 1–1 process for scattering states separated in energy by $\pm(\epsilon_{ph} = 2\hbar v_s k_{\parallel})$, representing the maximum acoustic phonon energy for a given $k_{\parallel}$. These results, summarised in table 1, show a deviation of typically only 1% from the values for $\epsilon_{ph} = 0$. The 1-band effective mass calculation yields the same fixed values for the AC scattering matrix elements as those shown in figure 2 for NPO scattering, and therefore serves as a reasonable approximation for the intraband AC processes described above (see figure 8). However, for AC 2–2 and AC 4–4 scattering, a second (broken) curve is shown on figure 8. This corresponds to scattering between equal energy states lying on opposite sides of the off-zone-centre energy minimum in each of bands 2 and 4. For each process the two curves coincide at the wavevector of the energy minimum; $k_{\parallel} = 0.015$ Å^{-1} in band 2, and 0.021 Å^{-1} in band 4, but the matrix elements for these 'cross valley' transitions fall off as $k_{\parallel}$ shifts away from these points, since the scattering states become less similar in character.

The matrix elements for interband AC scattering are all considerably smaller than the intraband results. As in the case of NPO scattering, the most important interband processes are those involving adjacent, anticrossing bands, and these have matrix elements which again

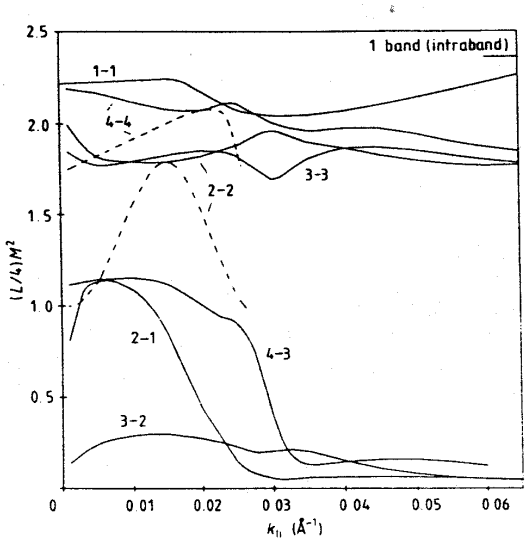

Figure 8. Matrix elements squared for AC scattering, as a function of the in-plane wavevector of the lower energy state. The broken curves are the results for the 'cross-valley' processes in bands 2 and 4, ~~and the full curves represents the 1-band effective mass result for intraband scattering~~.

Table 1. Matrix elements squared for AC 1–1 scattering. Results are given for the elastic case ($\epsilon_{ph} = 0$), and for a separation of the scattering states by $\epsilon_{ph} = \pm 2\hbar v_s k_{\parallel}$, $\approx 0.5k_{\parallel}$ for holes in GaAs, with $k_{\parallel}$ in units of 10^{-2} Å^{-1}

k (× 10^{-2} Å^{-1})	ϵ_{ph} (meV)	(L/4) M²
0.5	0.0	2.196
	0.25	2.196
	−0.25	2.196
1.0	0.0	2.217
	0.5	2.220
	−0.5	2.212
2.0	0.0	2.177
	1.0	2.094
	−1.0	2.165
3.0	0.0	2.044
	1.5	2.032
	−1.5	1.999
4.0	0.0	2.068
	2.0	2.081
	−2.0	2.051

SST 271-7

exhibit a distinct change of magnitude when the wavevector of one of the scattering states traverses an anticrossing region.

4. Conclusion

We have presented a calculation of hole–phonon scattering matrix elements in a quantum well. The calculation is based on a 4 band $\boldsymbol{k}\cdot\boldsymbol{p}$ scheme, and therefore enables us to examine the effects of heavy hole–light hole mixing on phonon scattering in the quantum confined valence band system. We observe strong dependences of the matrix elements for optical phonon scattering on the in-plane wavevectors of the scattering states, associated with changes in the character of these states near the anticrossing regions in the bandstructure. The largest matrix elements are those for intraband scattering, with the most important interband processes being those involving adjacent and anticrossing subbands. For acoustic phonon scattering, the matrix elements for the intraband processes are relatively insensitive to the carrier wavevectors, and, in this case only, the 1-band effective mass model gives a reasonable approximation to the results. However, an additional set of intraband processes exists, due to the presence of off-zone-centre energy minima in certain bands, and these processes have a distinct wavevector dependence. Interband scattering via acoustic phonons appears to be relatively unimportant.

We may expect to find trends similar to those discussed above in the hole–phonon scattering rates, but with modifications introduced by the density of states $D_{n'}(k'_{\parallel})$. Results for these scattering rates will be reported as part of a forthcoming publication.

Acknowledgments

RWK, RIT and ACGW acknowledge financial support from SERC for the period of this work, the latter holding a CASE award with Plessey Research Caswell Ltd.

References

[1] Price P J 1981 *Ann. Phys. NY* **133** 217
[2] Ridley B K 1983 *J. Phys. C: Solid State Phys.* **15** 5899
[3] Riddoch F A and Ridley B K 1983 *J. Phys. C: Solid State Phys.* **16** 6971
[4] Chang Y C and Schulman J N 1983 *Appl. Phys. Lett.* **43** 536
[5] Chang Y C and Schulman J N 1985 *Phys. Rev.* B **31** 2069
[6] Kelsall R W 1989 PhD Thesis University of Durham unpublished
[7] Babiker M 1986 *J. Phys. C: Solid State Phys.* **19** L339
[8] Schuurmans M F H and 't Hooft G W 1985, *Phys. Rev.* B **31** 8041
[9] Eppenga R, Schuurmans M F H and Colak S 1987 *Phys. Rev.* B **36** 1554
[10] Ridley B K 1988 *Quantum Processes in Semiconductors* 2nd edn (Oxford: Clarendon)
[11] Frölich H 1937 *Proc. R. Soc.* A **160** 230
[12] Callen H B 1949 *Phys. Rev.* **76** 1394